COORDINATED NANOSIMS AND TEM ANALYSIS OF A LARGE ^{26}MG-RICH AGB SILICATE FROM THE METEORITE HILLS 00426 CR2 CHONDRITE. A. N. Nguyen[1,2], L. P. Keller[2], and Z. Rahman[1,2]. [1]Jacobs, NASA Johnson Space Center, Houston TX 77058 (lan-anh.n.nguyen@nasa.gov). [2]ARES, NASA Johnson Space Center, Houston TX 77058.

Introduction: Silicates are one of the most abundant presolar phases around evolved stars, in the interstellar medium (ISM), and in our Solar System. These grains afford the opportunity for O, Si, Mg, Fe, and Ca isotopic analyses to constrain stellar nucleosynthetic and mixing processes, and Galactic chemical evolution (GCE). While Mg and Fe isotopic studies have been successfully conducted on presolar silicates, isotopic analyses beyond O and Si are often hampered by the small grain sizes (average ~250 nm). This also makes coordinated mineral and chemical characterization challenging. These studies provide insight into the dust condensation conditions as well as subsequent alteration in the ISM and/or the Solar System. TEM studies of presolar silicates have shown that they are much more mineralogically and chemically diverse than other presolar phases [1 and references therein]. Large (>500nm) presolar silicate grains are rare, but they allow for detailed isotopic, mineral, and chemical characterization. We identified a large presolar silicate grain in the MET 00426 CR2 chondrite and report the O, Si, Mg, and Fe isotopic compositions and TEM study of this grain.

Sample and Methods: A ~0.4 g piece of MET 00426 was disaggregated by repeated freeze-thaw and ultrasonication. Soluble organic matter was removed and ~0.1-1.5 μm-sized silicate grains were separated by repeated centrifugation in isopropanol/water. The grains were deposited from suspension onto clean Au foil.

NanoSIMS Analysis. Dense grain areas were selected for O and Si isotopic analysis using the JSC NanoSIMS 50L. A 1.4 pA Cs^+ primary ion beam was rastered over 20 μm fields of view for 20 planes. An electron flood gun was used for charge compensation. Solar System matrix grains served as the isotopic standard. A total area of 41,230 μm^2 was analyzed and 38 O anomalous grains were identified. One region showed two Si- and MgO-rich areas having the same anomalous O isotopic ratio (Fig. 1). Examination of the area in the SEM revealed a single, large 1.5×0.75 μm grain with isotopically normal material draped across the center (Fig. 2).

Further NanoSIMS Mg and Fe isotopic analysis was conducted on the anomalous grain (2_8_4) using the duoplasmatron primary ion beam source. To reduce isotopic dilution and obtain more accurate isotopic ratios, a focused Cs^+ beam was used to carefully sputter away the overlying isotopically solar material. The Si and MgO signals were monitored to assess when the relatively Si- and MgO-poor solar material was sputtered away. A ~2.4 pA O^- primary ion beam was then rastered over an 11 μm field of view around grain 2_8_4. Positive secondary ions of ^{24}Mg, ^{25}Mg, ^{26}Mg, ^{52}Cr, ^{54}Fe, ^{56}Fe, and ^{57}Fe were simultaneously measured. Surrounding matrix grains served as isotopic standards. Chromium-52 was measured to correct for the unresolvable interference of ^{54}Cr on ^{54}Fe. Aluminum-27 was subsequently measured along with the Mg isotopes.

TEM Characterization. An electron transparent cross-section of grain 2_8_4 was prepared by focused ion beam (FIB– FEI Quanta 3D FEG dual beam) milling. E-beam deposited carbon was placed over the grain to serve as protection and as a marker for grain identification during section thinning. An ion-beam deposited C strap was then placed over the entire 6-μm long section, which was lifted out, attached to a TEM grid, and thinned to electron transparency. The JSC JEOL 2500 field-emission scanning TEM was used to image the grain and determine its mineralogy and chemical composition. Elemental maps were acquired with JEOL Si-drift detector energy-dispersive X-ray analyses using a 2 nm incident probe. Grain crystallinity was assessed by electron diffraction and dark-field imaging.

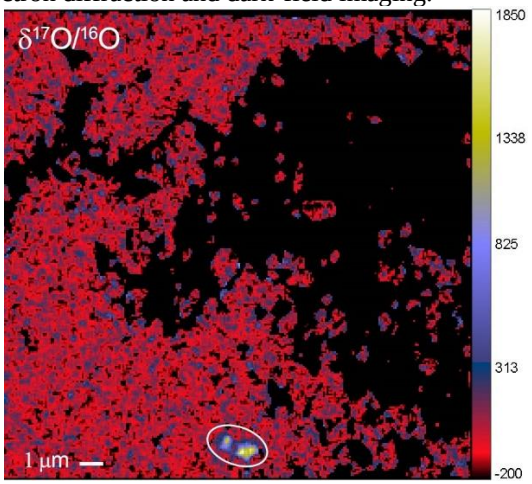

Figure 1. NanoSIMS $\delta^{17}O/^{16}O$ ratio image of an analyzed region of MET 00426 matrix grains. What appeared to be two isotopically anomalous grains (circled) was actually one large silicate that was partially covered by isotopically normal material.

Results and Discussion: Grain 2_8_4 is ^{17}O-rich and ^{18}O-poor ($\delta^{17}O$ = 1510 ± 120‰; $\delta^{18}O$ = -170 ± 30‰) with normal Si isotopic composition. These compositions fall into the Group 1 classification of presolar

O-rich grains and are consistent with formation in a ~1.5 $M_\odot$ asymptotic giant branch (AGB) star of solar metallicity. The grain is also ^{25}Mg-poor and ^{26}Mg-rich (δ^{25}Mg = -31 ± 5‰; δ^{26}Mg = 162 ± 5‰) with normal Fe isotopic composition. Similar Mg isotopic compositions have been observed in a few other Group 1 silicates [2].

The Mg isotopic ratios of many AGB silicates and oxides mainly reflect the initial compositions of their parent stars as determined by GCE [3,4,5,7]. During the evolution of low-mass AGB stars, the Mg isotopes are altered by multiple nuclear reactions but the predicted enrichment in ^{26}Mg is <20‰ without contributions from ^{26}Al decay and <80‰ with ^{26}Al decay [5]. The ^{25}Mg depletion of 2_8_4 could reflect a low metallicity source, but this is inconsistent with the ^{18}O/^{16}O ratio. Moreover, the measured ^{26}Mg enrichment is greater than predicted for AGB nucleosynthesis.

Large excesses in ^{26}Mg observed in Group 1 and 2 oxides and silicates without corresponding ^{25}Mg excesses have been attributed to the in situ decay of ^{26}Al ($t_{1/2}$ = 7.1×10^5 yr) [e.g., 3,5-7]. The Group 2 grains also have large ^{18}O depletions. The extra mixing processes cool bottom processing (CBP) [8] and hot bottom burning (HBB) [9] have been evoked to explain the ^{18}O deficits and high inferred ^{26}Al/^{27}Al of these grains. In CBP, the production of ^{26}Al depends on the maximum temperature reached by the envelope, while ^{18}O destruction depends on the mass circulation rate. The ^{26}Mg enrichment of grain 2_8_4 could be explained if the parent stellar envelope reached very high temperatures but had a low mass circulation rate. However, to have C/O <1 so that O-rich phases condense, the CBP model requires mass circulation rates greater than ~10$^{-6.4}$ $M_\odot$/yr which consequently produces lower ^{18}O/^{16}O than measured in 2_8_4. HBB also cannot explain the isotopic compositions of 2_8_4 because it occurs in intermediate-mass stars rather than low-mass, produces large ^{25}Mg excesses which is not observed, and greatly depletes ^{18}O.

The inferred initial ^{26}Al/^{27}Al ratio of 2_8_4 was determined by projecting the Mg isotopic ratio back to the GCE line as described by [5] to obtain the amount of radiogenic ^{26}Mg. Grain 2_8_4 has a very low Al/Mg ratio of 0.001 (upper limit) as determined by TEM-EDX and its inferred initial ^{26}Al/^{27}Al ratio of 21 ± 6.6 is extremely high. Presolar oxides have ^{26}Al/^{27}Al ratios <0.1 [7]. 2_8_4 did not condense appreciable amounts of Al and only contains a small amount of radiogenic ^{26}Mg, if any. The ^{25}Mg-poor and ^{26}Mg-rich composition of 2_8_4 could be explained by more efficient ^{26}Mg production and mixing into the envelope in AGB stars than predicted. Alternatively, the data can be explained by local isotopic heterogeneity in the ISM due to incomplete mixing of supernova (SN) ejecta. Indeed, many SN oxides and silicates are ^{26}Mg-rich and ^{25}Mg-poor due to mixing of material from the He/N and He/C shells with the H envelope [7, 10]. This incomplete mixing could have altered the initial Mg isotopic composition of the parent star of 2_8_4 from GCE model predictions. However, this would require little contribution from the ^{18}O-rich He/C zone. Heterogeneity in the ISM was also invoked to explain the Mg isotopic compositions of other presolar silicates and oxides [4,7,11].

TEM analysis indicates 2_8_4 is a single crystal of essentially pure forsterite (Fo 99.8) with a few dislocations but no radiation damage in the form of rims or tracks (Fig. 2). The uppermost surface of the grain shows a damaged rim and sputter redeposited material from the NanoSIMS analyses. Most other presolar forsterite grains have greater Fe-contents that were attributed to primary condensation [1 and references therein]. Another large presolar forsterite from MET 00426 has a low Fe-content (Fo 98) similar to 2_8_4 [12]. The low Fe-contents of these two presolar forsterite grains suggest condensation at high temperatures or at comparatively reduced conditions. It is often difficult to discern NanoSIMS ion beam damage from radiation damage in the ISM in small presolar silicates. However, both large presolar forsterites show no evidence for ISM processing, suggesting short ISM residence times.

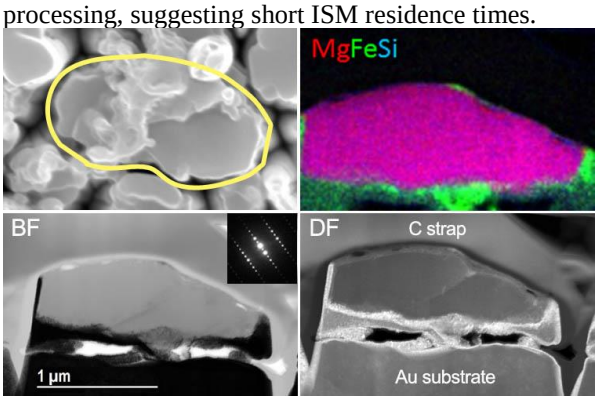

Figure 2. (upper left) Plane view of 2_8_4 (outlined) before removal of isotopically solar material across the grain's center. Composite elemental map, diffraction pattern, and bright-field and dark-field STEM images.

References: [1] Nguyen A. N. et al. (2016) *ApJ, 818*, 51-67. [2] Verdier-Paoletti M. J. et al. (2019) *MAPS*, #6433. [3] Kodolányi J. et al. (2014) *GCA, 140*, 577-605. [4] Hoppe P. et al. (2018) *ApJ, 869*, 47-59. [5] Zinner E. et al. (2005) *GCA, 69*, 4149-4165. [6] Nguyen A. N. and Zinner E. (2004) *Science, 303*, 1496-1499. [7] Nittler L. R. et al. (2008) *ApJ, 682*, 1450-1478. [8] Nollett et al. (2003) *ApJ, 582*, 1036-1058. [9] Lugaro M. et al. (2017) *Nature Astronomy, 1*, 0027. [10] Nguyen A. N. and Messenger S. (2014) *ApJ, 784*, 149. [11] Leitner J. et al. (2019) *LPSC L*, #2090. [12] Nguyen A. N. et al. (2017) *MAPS*, #6332.